Earth and Planetary Science Letters 453 (2016) 223–233

Contents lists available at ScienceDirect

Earth and Planetary Science Letters

www.elsevier.com/locate/epsl

An alternative model for $CaCO_3$ over-shooting during the PETM: Biological carbonate compensation

Yiming Luo [a], Bernard P. Boudreau [a,*], Gerald R. Dickens [b], Appy Sluijs [c], Jack J. Middelburg [c]

[a] Department of Oceanography, Dalhousie University, Halifax, Nova Scotia B3H4J1, Canada
[b] Department of Earth Sciences, Rice University, Houston, Texas 77005, USA
[c] Department of Earth Sciences, Faculty of Geosciences, Utrecht University, Utrecht, Netherlands

ARTICLE INFO

Article history:
Received 22 February 2016
Received in revised form 10 July 2016
Accepted 8 August 2016
Available online 30 August 2016
Editor: H. Stoll

Keywords:
PETM
ocean acidification
carbonate compensation
carbonate export
$CaCO_3$ over-shooting

ABSTRACT

Decreased $CaCO_3$ content of deep-sea sediments argues for rapid and massive acidification of the oceans during the Paleocene–Eocene Thermal Maximum (PETM, ∼56 Ma BP). In the course of the subsequent recovery from this acidification, sediment $CaCO_3$ content came to exceed pre-PETM levels, known as over-shooting. Past studies have largely attributed the latter to increased alkalinity input to the oceans via enhanced weathering, but this ignores potentially important biological factors. We successfully reproduce the $CaCO_3$ records from Walvis Ridge in the Atlantic Ocean, including over-shooting, using a biogeochemical box model. Replication of the $CaCO_3$ records required: 1) introduction of a maximum of ∼6500 GtC of CO_2 directly into deep-ocean waters or ∼8000 GtC into the atmosphere, 2) limited deep-water exchange between the Indo-Atlantic and Pacific oceans, 3) the disappearance of sediment bioturbation during a portion of the PETM, and 4) most central to this study, a ∼50% reduction in net $CaCO_3$ production, during acidification. In our simulations, over-shooting is an emergent property, generated at constant alkalinity input (no weathering feedback) as a consequence of attenuated $CaCO_3$ productivity. This occurs because lower net $CaCO_3$ production from surface waters allows alkalinity to build-up in the deep oceans (alkalinization), thus promoting deep-water super-saturation. Restoration of $CaCO_3$ productivity later in the PETM, particularly in the Indo-Atlantic Ocean, leads to greater accumulation of $CaCO_3$, ergo over-shooting, which returns the ocean to pre-PETM conditions over a time scale greater than 200 ka.

1. Introduction

The Paleocene–Eocene Thermal Maximum (PETM), a transient climate-warming event that began ∼56 Ma, has generated intense research interest. Over a geologically brief interval (<20 kyr), Earth's surface warmed by ∼6 °C, massive amounts of CO_2 entered the ocean and atmosphere, and ecosystems, both terrestrial and marine, changed dramatically (McInerney and Wing, 2011). The PETM seemingly provides our best past example for understanding future ocean acidification (Zachos et al., 2005; Zeebe and Ridgwell, 2011).

The calcite snowline delineates the ocean depth where sediments are first $CaCO_3$ free (Zeebe and Westbroek, 2003; Boudreau et al., 2010a). Sedimentary records indicate that, prior to the PETM, the calcite snowline was positioned >4200 m paleo-depth in the south-central Atlantic and near 3400 m in the Pacific (Zeebe et al., 2009; Cui et al., 2011). The onset of the PETM was marked by a transient decrease in the $CaCO_3$ content of bottom sediments and a rise in the snowline in the Atlantic by at least 2000 m, while the Pacific snowline appears to have shallowed by <500 m. These adjustments have been attributed to significant CO_2 input to the oceans over a period of many millennia (Dickens et al., 1997; Zachos et al., 2005; Ridgwell, 2007; Zeebe and Zachos, 2007; Zeebe et al., 2009; Cui et al., 2011; McInerney and Wing, 2011; Zeebe and Ridgwell, 2011), as well as changes in circulation (Zeebe et al., 2009). The origin of the CO_2, which was depleted in ^{13}C, has been attributed to various sources, including oxidation of methane in the ocean (Dickens et al., 1995), or the oxidation of organic matter on land (e.g., DeConto et al., 2012).

Irrespective of source, massive injection of CO_2 into the ocean-atmosphere system caused increased dissolution of biogenic $CaCO_3$ at and within the seafloor:

$$CaCO_3 + CO_2 + H_2O \rightarrow Ca^{2+} + 2HCO_3^- \quad (1)$$

* Corresponding author.
E-mail address: bernie.boudreau@dal.ca (B.P. Boudreau).

http://dx.doi.org/10.1016/j.epsl.2016.08.012
0012-821X/

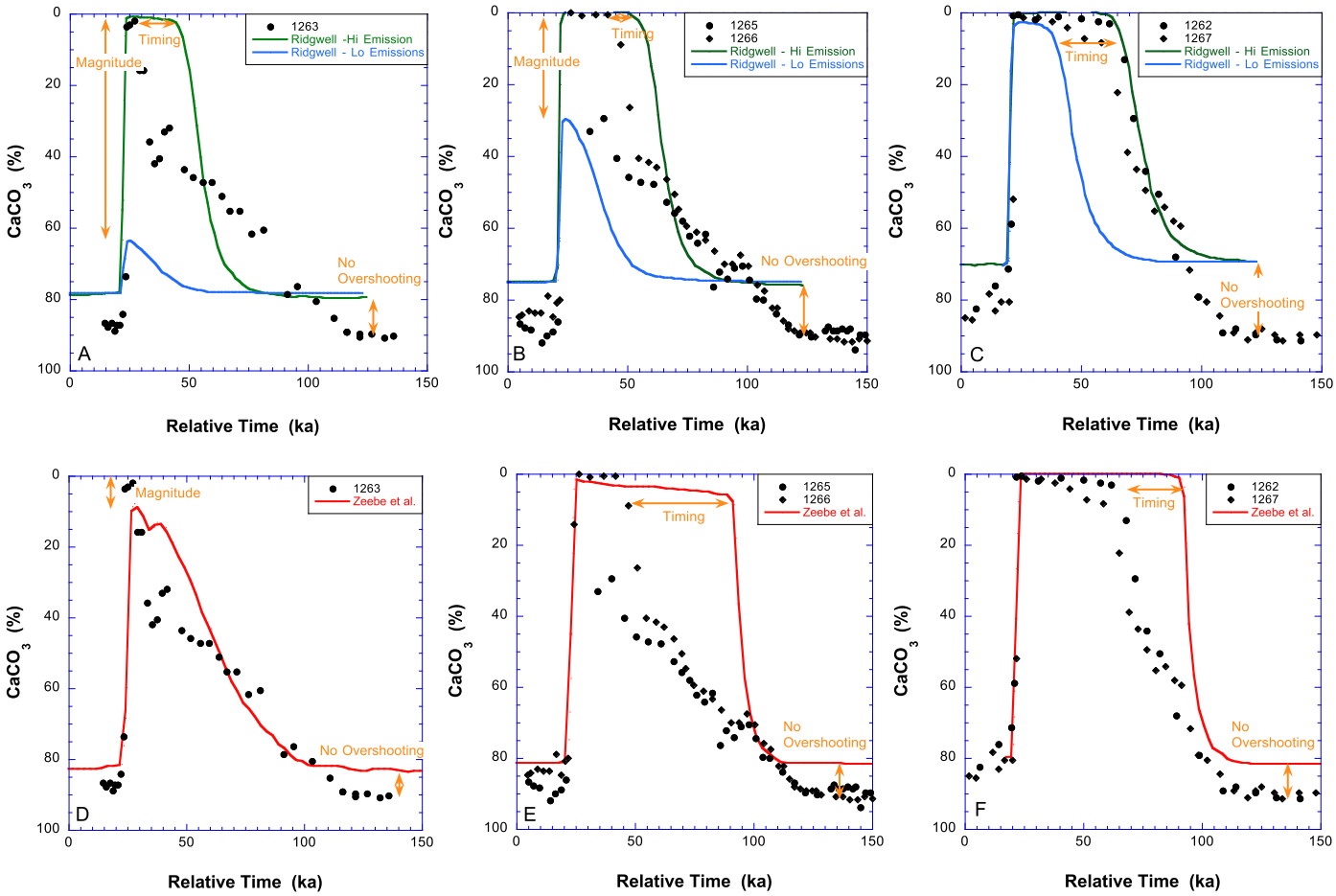

Fig. 1. Plots of the recorded $CaCO_3$ time series (data) at Walvis Ridge sites at 1500 m paleo-depth (1263), 2600 m paleo-depth (1265, 1266) and 3600 m paleo-depth (1262, 1267) presented in Zeebe et al. (2009). Panels **A**, **B** and **C** show the results of the Ridgwell (2007) model, and Panels **D**, **E** and **F** display the results from the Zeebe et al. (2009) model.

This additional $CaCO_3$ dissolution neutralized the added CO_2, returning oceanic chemistry towards its original state, a process classically termed *carbonate/calcite compensation* (Zeebe and Westbroek, 2003; Boudreau et al., 2010a). Compensation is recorded as a temporal drop in the $CaCO_3$ content of sediments at a given (paleo-)oceanographic depth, and a consequent rise in the snowline depth with time.

Available $CaCO_3$ records indicate that after initial shallowing, the PETM snowline at Walvis Ridge (south-central Atlantic) – Fig. 1 – must have moved downward substantially, termed *over-shooting* (also sometimes called *over-deepening*). The exact position of the snowline is not preserved in available records and can only be inferred. The Walvis Ridge PETM records (Zachos et al., 2005) show, for example, that at 1500 m paleo-depth, $CaCO_3$ was 88% pre-PETM, but reached 91% by 110 ka after PETM onset (ka PO, hereafter), while at 2600 m, the change was from 83.5% to 92%, and that at 3600 m was from 75% to 92%. The preservation of components within this biogenic carbonate shows that over-shooting represents enhanced preservation (Kelly et al., 2010) and implies substantial deepening of the snowline. The Pacific snowline may also have exhibited minor over-shooting, as observed in the records of $CaCO_3$ and planktonic foraminifera at ODP Site 1215 (Leon-Rodriguez and Dickens, 2010). The snowlines then appear to have returned to pre-PETM positions over a period >200 ka.

Biogeochemical modeling offers a means to investigate and test hypotheses about the causes of these phenomena, e.g., Dickens et al. (1997), Ridgwell (2007), Panchuk et al. (2008), Kump et al. (2009), and Zeebe et al. (2009). These models have contributed fundamentally to our understanding of the PETM, but they have not reproduced quantitatively the $CaCO_3$ records spanning the PETM – see Fig. 1, as examined in detail below. Understanding what happened during PETM acidification requires that our hindcasts/retrodictions account for the *magnitude* of the predicted drop in $CaCO_3$ content with the initial acidification, (2) the *timing* of the resumption of $CaCO_3$ deposition, and (3) as highlighted in this paper, the presence of *over-shooting* in the period after 100 ka PO (Fig. 1).

A failure to hindcast the magnitude and timing of the changes in $CaCO_3$ records raises questions regarding our understanding of the cause(s) and control(s) of PETM acidification. Likewise, a lack of over-shooting in a model's results means that the identity and functioning of the recovery process in the oceans remains undefined. Earth System Science-based models have indeed managed to hindcast over-shooting, e.g., Dickens et al. (1997), Kump et al. (2009), Cui et al. (2011), and Penman et al. (2016). The cause of over-deepening in such models is linked to increased weathering (Zeebe and Zachos, 2013; Penman et al., 2016), due to high atmospheric CO_2 and temperatures (i.e., weathering feedback), and a resulting increased alkalinity input to the oceans. Other well-regarded models simply lack over-shooting altogether, e.g., Ridgwell (2007) and Zeebe et al. (2009) – Fig. 1.

The implicit acceptance of increased weathering/alkalinity input as the cause of over-shooting is qualitatively supported by proxy evidence for weathering. The marine $^{187}Os/^{188}Os$ evolution during the PETM is characterized by a transient increase to more radiogenic values (Ravizza et al., 2001). It remains unclear, how-

ever, how this signal scales quantitatively to alkalinity input, which leaves room for alternative explanations.

All previous modeling studies have overlooked the potentially important role of biology in creating or contributing to over-shooting. Biology can significantly impact the carbonate chemistry of the oceans during acidification events, as seen in the model results from Zeebe and Westbroek (2003), Ridgwell and Hargreaves (2007), and Boudreau et al. (2010b). Experimental evidence indicates that the production of $CaCO_3$ in the surface ocean will decrease in response to ocean acidification (e.g., Riebesell et al., 2000; Orr et al., 2005; Riebesell, 2008; Waldbusser et al., 2014) and such a drop in production should lead to diminished $CaCO_3$ export from the surface to the deep waters and, consequently, a decline in alkalinity removal from the oceans, allowing its build-up. The question then becomes, could a reduction in net $CaCO_3$ production contribute to over-shooting?

The aim of this paper is to explore this question using a simple biogeochemical box model, all while employing the data in Fig. 1 to test/falsify the model output and conclusions. Our goal is not to disprove the weathering-alkalinity flux hypothesis, but rather to determine the viability of a biological alternative. Consequently, we simply omit weathering feedbacks and see what else can occur to explain the data.

2. Modeling carbonate dynamics during the PETM

2.1. Background

As stated above, the snowline is a compositional boundary (depth) in the oceans, separating sediments above that contain measurable $CaCO_3$ (calcite) from those below that contain little measurable $CaCO_3$ (Zeebe and Westbroek, 2003). In a steady state ocean, the snowline corresponds to the calcite/carbonate compensation depth (CCD), where the rain of biogenic $CaCO_3$ reaching the seafloor is exactly balanced by the rate of dissolution. The often encountered term lysocline was coined to designate the depth where foraminiferal calcite tests are first observed to exhibit clearly the effects of dissolution; as explained by Boudreau et al. (2010a), the lysocline is then a subjective, observational feature that has no dynamic meaning, although it is sometimes equated with either the CCD or the snowline. Lysocline is not used further in the current paper.

The present-day snowline/CCD is geographically variable in its depth, broadly shallowing from the Atlantic Ocean into the Pacific Ocean, which reflects the greater under-saturation of the latter ocean. During transient acidification (past or future), the snowline and CCD do not correspond (Boudreau et al., 2010a) because the CCD represents an interface of a dynamic balance and will shift upwards immediately upon acidification. In contrast, the snowline will only move upward as all the $CaCO_3$ contained in the biologically influenced portion of surface sediments is dissolved by acidification and that delay can be as much as 75 ka later than an upward CCD shift. Therefore, dissolution of previously deposited $CaCO_3$ (carbonate compensation) slowly restores the equivalence of the CCD and snowline.

A major issue confronts our understanding of snowline movement and $CaCO_3$ accumulation across the PETM. Very few locations have been drilled where the paleo-water depth, tectonic history, and core recovery are amenable to reconstructing the $CaCO_3$ snowline over time (Cui et al., 2011; Slotnick et al., 2015). In general, the available records (Fig. 1) strongly suggest a shallower overall snowline in the latest Paleocene relative to present-day, a shoaled snowline from the central Atlantic to central Pacific over much of the early Paleogene, similar to present-day, and amplified dissolution and over-shooting across the PETM in the Atlantic. While these "facts" have been suggested for over 15 yr, Walvis Ridge (Fig. 2), with multiple sites cored along a depth transect, remains the only location amenable to detailed modeling of $CaCO_3$ accumulation during the PETM.

2.2. Past studies

Previous modeling of CCD and snowline movements during PETM acidification has required an accounting of both the changing carbonate chemistry of the oceans and the composition of sediments with oceanographic depth. Dickens et al. (1997) first employed a carbon-cycle box model to advance that the PETM $\delta^{13}C$ records at ODP Sites 690 and 865 were consistent with a release and oxidation of ∼840 GtC from seafloor CH_4 hydrate systems, when started with (modern) pre-industrial conditions. This carbon mass is too small, as realized in later works (Dickens, 2001; Carozza et al., 2011); nevertheless, these model results do display a rise in carbonate saturation depth during CO_2 release and subsequent over-shooting. Ridgwell (2007), using the GENIE-1 model, determined that diminished bioturbation in deep-ocean sediments was necessary to explain the $CaCO_3$-free sediments at Walvis Ridge in the Atlantic Ocean, in addition to CO_2 release – see Fig. 1 (top panels). He further found that the changes in the $CaCO_3$ record were more consistent with an input of 9000 GtC, rather than 4500 GtC of CO_2. Panchuk et al. (2008) used the same model to place a lower limit of 6800 GtC on the total CO_2 release into the oceans, while Cui et al. (2011) again employed it to place limits on CO_2 release between 2500 and 13000 GtC, depending on the nature of the source. Kump et al. (2009), again employing GENIE-1, were able to relate over-deepening in the PETM to increased alkalinity input to the oceans from enhanced continental weathering. Zeebe et al. (2009), using the LOSCAR model and the $\delta^{13}C$ record at Walvis Ridge, predicted that 3000 GtC of CO_2 were released in the first 5 ka from PETM onset (ka PO, hereafter) directly into ocean waters from oxidized methane, followed by a release of 1480 GtC over the next ∼65 ka – see Fig. 1 (bottom panels). Penman et al. (2016) have recently modeled carbonate data at site U1409 and hindcast overshooting in their results from the cGENIE model, again driven by a weathering feedback.

Further hindcasts have been made by Alexander et al. (2015), based on a 3-D climate/ocean chemistry model (UVic ESCM), which attributes the reduced preservation in the Atlantic versus the Pacific to transient build-up and release of corrosive water in the North Atlantic; however, that paper provides no quantitative predictions regarding $CaCO_3$ content or snowline movement.

2.3. A new simple model

Our model (Fig. 3) is based on Boudreau et al. (2010b), which is an extended Harvardton–Bear three-box model of the oceans with an added, attached sediment reservoir. Our present model is simply two such models, one for the Indo-Atlantic and one for the Pacific oceans, linked together – a configuration justified below.

The choice of dividing the world's ocean into only four boxes might, at first, appear to be a too coarse-grained approach. However, the earlier Boudreau et al. (2010b) model has been tested against the results of other box models and 3D biogeochemical models listed in Archer et al. (2009) for the present-day ocean and its future long-term acidification. Even though our model was found to produce highly comparable results, we recognize that model compatibility in today's oceans does not guarantee the same for the PETM. Nevertheless, our present model can reproduce retrodictions of the pre-PETM oceans (Heinze and Ilyana, 2015), which closely resemble those in Ridgwell (2007) and Zeebe et al. (2009), as will be seen by comparing the pre-PETM lines in Fig. 1 with our later results. We agree that our approach ignores chemical differences that may have existed between the Atlantic and

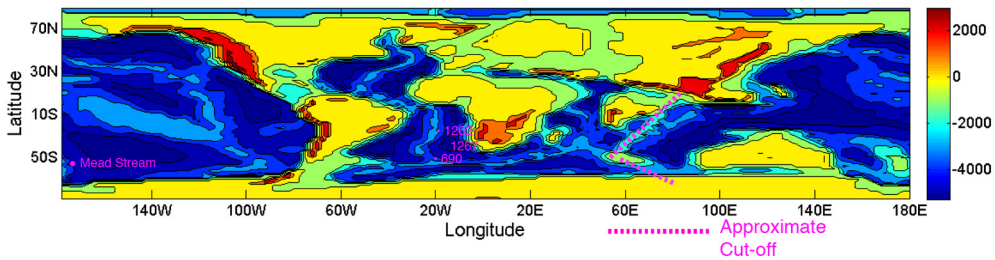

Fig. 2. Bathymetry of the PETM oceans as reconstructed by Bice and Marotzke (2001), showing the approximate position of our proposed cut-off for deep-water exchange between the Indo-Atlantic and Pacific Oceans. The approximate positions of Walvis Ridge Sites 1262–1267, as well as ODP Site 690 (Maud Rise) and the Mead Stream Sites, are indicated on this map.

Indian Oceans or even within the Atlantic Ocean; thus, we adopt the position that such lateral differences will not alter the basic findings of our paper.

Our approach also assumes that the carbonate chemistry of the deep oceans and the low-latitude and high-latitude surface oceans can be assumed to be homogeneous, to a reasonable degree of accuracy. To this point, the detailed hindcasts supplied by Heinze and Ilyana (2015) show fairly uniform pre-PETM ocean chemistries below 1000 m, with ∼20% maximum gradients between 200 and 1000 m in the Atlantic Ocean. Adoption of our box model does not seem contra-indicated by this level of spatial variability. Whereas Heinze and Ilyana (2015) hindcast much larger variability for surface water (<200 m), these surficial spatial patterns play no material role in the issues addressed herein. We also advance that the primary chemical dichotomy that existed during the PETM was the contrast between the Indo-Atlantic and the Pacific Oceans, and that can be captured by a four-box ocean model.

Our model accounts for the carbonate alkalinity (CAlk) and total dissolved CO_2 (ΣCO_2) in each water box, as forced by inputs from the atmosphere, rivers, and sediments; as well, it calculates the amount of $CaCO_3$ in sediments at every ocean depth – see Appendix A for details. The reactions within an ocean that affect CAlk and ΣCO_2 include net production of $CaCO_3$ from the surface oceans (B) and its dissolution into the deep boxes (B_D), which depends on the saturation level, as well as net organic matter production from the surface boxes and oxidation in the deep boxes (P). (The net production B is the amount of $CaCO_3$ produced in shallow waters that sinks into the deep sea, sometimes called the export flux.) Finally, our model does not contain shallow water carbonates and refers only to the pelagic ocean. As such the riverine flux refers not to the amount actually coming down rivers, but the portion that reaches the pelagic ocean after shallow water processes remove their required alkalinity. Finally, as indicated above, we employ the results from Heinze and Ilyana (2015) to set the initial chemical conditions for our own work.

3. The data and its treatment

We employed only the $CaCO_3$ records (Fig. 1) from the Walvis Ridge sites (Fig. 2) for our study. Walvis Ridge provides data at different paleo-depths within a single geographically and geochemically contiguous area, which is not the case anywhere else where the PETM has been sampled. This situation permits us to fix all free model parameters with the $CaCO_3$ record at one depth (we use the shallowest depth – 1500 m), and then make predictions with no parameter adjustments at the other two depths.

The common practice of applying a model to the $CaCO_3$ data at a number of different, widely spaced sites across the oceans is highly informative with respect to establishing variability of parameters. For example, our available free parameters can be used to create correspondence between our model output and the $CaCO_3$ records at Site 690 in the South Atlantic Ocean (Appendix A). Nonetheless, this procedure cannot provide falsification, and falsification is at the heart of our methodology. Thus, for the purposes of the current paper, i.e., establishing the viability of new mechanisms, we call on multiple-depth testing solely.

We make no direct use of carbon isotopic data in the above described analysis, such as employed in Zeebe et al. (2009) or Cui et al. (2011). These data, while extremely valuable, cannot aid in matching the output of our model to the $CaCO_3$ records. Our chosen approach allows us to obtain the magnitude of the release without knowing the exact source. However, carbon isotopic data can be crucial in helping to identify the source of the CO_2 that affected the PETM, and one attempt at fitting this data is illustrated in Appendix A.

We do not focus on the nature of the CO_2 source in the modeling, but we do test the effects of where CO_2 is released. This is because direct injection into the deep sea, such as through seafloor CH_4 release and oxidation, could impact carbonate accumulation differently than direct injection into the atmosphere. If all other processes are fixed, this spatial dichotomy of the CO_2 source produces modestly different predictions of the $CaCO_3$ records, as shown in Appendix A. Consequently, the results reported here focus on those generated with deep-sea CO_2 release, similarly to previous work (e.g., Zeebe et al., 2009).

Our box model demands ocean bathymetry to calculate the amount of water in each box, and a hypsographic curve to determine the depth-dependent saturation state of the deep ocean basins, the positions of the critical carbonate depths (Boudreau et al., 2010a, 2010b), and the distribution of $CaCO_3$ with depth. Bice and Marotzke (2001) and Herold et al. (2014) provide bathymetries for the PETM, but given the timing of this research, only the Bice and Marotzke (2001) data were available and used in our model (Fig. 2).

Both Bice and Marotzke (2001) and Herold et al. (2014) indicate significant bathymetric highs separating the western side of the Atlantic from the eastern side of the Pacific. Specifically, Drake Passage was closed (Scher and Martin, 2006), and while the Isthmus of Panama was open, it was likely only a shallow water connection; this is because, during the late Paleocene, the Caribbean large igneous province (LIP) was at the location of the present isthmus (Montes et al., 2012), and intense arc magmatism was occurring in this region (Wegner et al., 2011).

More interestingly, bathymetric reconstructions contain bathymetric highs in the Central Indian Ocean (Bice and Marotzke, 2001; Herold et al., 2014; Baatsen et al., 2016), which would have separated the western Indo-Atlantic deep waters from the eastern Indo-Pacific deep-waters. The evidence for such shallow barriers in the Early Paleogene is compelling and comes from multiple sources. For example, studies of ocean drilling sites on Kerguelen Plateau and Broken Ridge indicate that they formed a contiguous, partially sub-areal, igneous province (Weis et al., 1991; Wallace et al., 2002), slightly south of 50°S. Two-thirds of Ninetyeast Ridge (north of ODP Site 757) had formed (Nobre Silva et al., 2013), and it was much shallower than today (Weissel et al., 1991). Collectively, therefore, Kerguelen Plateau, Broken Ridge,

Ninetyeast Ridge, and the sub-Indian continent constituted a major separation between deep water in the Indian and Pacific basins. Evidence for at least partial oceanographic isolation also comes from neodymium isotopes of lower Paleogene sediment (Thomas et al., 2003; Abbott et al., 2016). These investigations show a strong dichotomy in Nd isotopic ratios between the Pacific ($\varepsilon_{Nd} = -3.5$ to -5.5) and Indo-Atlantic ($\varepsilon_{Nd} = -8$ to -10), and Abbott et al. (2016) stress that there "may not have been substantial exchange of deep waters" between these basins. Although greater detail regarding the location of barrier(s) between these basins is an intriguing direction for future research, this is not of fundamental importance for the purposes of our modeling, as it only dictates the relative volume of the water in our boxes.

Nevertheless, our starting conditions (Table A1 in Appendix A – Supplementary material) are similar to those in Zeebe et al. (2009), which includes the implicit assumption that the PETM circulation resembled that in today's oceans, including significant deep-water exchange – at least 25 Sv (Boudreau et al., 2010b). In addition, Ridgwell (2007) has demonstrated that bioturbation must severely diminish for $CaCO_3$-free sediments to accumulate at shallower depths, consistent with the record of the Walvis Ridge sediments (Bralower et al., 2014); therefore, we allow sediment mixing to be strongly attenuated during the initial CO_2 release, only to recover thereafter.

4. Results and discussion

Through model-data comparisons, a variety of failures and discrepancies allow re-evaluation of past assumptions from previous models, from which emerges a new perspective of how the oceans functioned during the PETM. We first explored various CO_2 release scenarios and amounts of water exchange between the Indo-Atlantic and Pacific Oceans. The pertinent aspects of these results are summarized in Figs. 4–7. Each of these figures shows our model predictions (solid curves) for the $CaCO_3$ time series at the three Walvis Ridge paleo-depths (i.e., 1500, 2600 and 3600 m) over the first 180 ka PO as functions of the total CO_2 released to the deep water, but fixed inter-ocean water exchange. (Note that the colors for the amounts of released CO_2 are consistent between panels and figures, and the red line, which is in every panel, can be used as a reference/datum between the plots; however, to avoid visual congestion, not every CO_2 release is replicated in every plot.) The four different figures arise because of different amounts of water exchange assumed between the Indo-Atlantic and Pacific Oceans (20 Sv in Fig. 4; 5 Sv in Fig. 5; 2 Sv in Fig. 6; 0 Sv, complete isolation, in Fig. 7). The plotted results represent a fraction of the hundreds of model runs made during this study, where values of all parameters were varied.

Model concordance with data could not be obtained if deep-water exchange ($U_{T,PA}$ and $U_{T,AP}$ in Fig. 3) of more than 2 Sv occurred between the Indo-Atlantic and Pacific Oceans; this is regardless of the amount of CO_2 released (i.e., from 2500 GtC to 10500 GtC). In other words, as shown in Figs. 4–6, no model line of one single color approximates the data at all three depths, simultaneously. However, the results in Fig. 7 with no exchange between the Indo-Atlantic and Pacific Oceans show that the $CaCO_3$ at the three paleo-depths can be well approximated by the red line in each of the three panels, i.e., a total release of 6500 GtC. In all tested cases, there remains ∼8 Sv of internal diapycnal mixing ($U_{M,A}$ in Fig. 3) within the Indo-Atlantic Ocean. We then repeated these calculations with initial releases of 1000 and 3000 GtC instead (not shown), but produced inferior approximations to the $CaCO_3$ data.

These results led us to conclude that two-way exchange between the Indo-Atlantic and Pacific Ocean basins must have been essentially zero during the PETM in order to explain the data and that the total CO_2 release into deep water was (about) 6500 GtC. Of this total amount, 2000 GtC was released initially in the first 5000 yr and 4500 GtC over the next 45000 yr. This two stage release is not unlike that proposed in Zeebe et al. (2009), though different in amounts liberated; they suggested 3000 GtC in about 5 ka followed by 1480 GtC over the next ∼50 ka. Furthermore, conformity to the data requires the injection to be skewed geographically. Specifically, with a total release of 6500 Gt, 1000 GtC are discharged into the Pacific, but 5500 GtC are input into the Indo-Atlantic. This dichotomy might relate to the proportional fraction of passive continental margins that might host extensive methane hydrates.

This estimated carbon release comes with a major caveat. Our model treats the ocean basins as homogeneous in composition (i.e., vast single boxes); however, lateral gradients could have existed, especially with diminished overturning circulation, such that conditions at Walvis Ridge could have been more acidified than other locations in the Atlantic or Indian oceans, for example at Maud Rise in the South Atlantic. Thus, the amounts determined above should be considered *maximum* estimates of CO_2 release.

We propose that the virtual lack of deep-water two-way exchange between the large oceans, as argued by our model results, was due to the presence during the PETM of a barrier to deep and mid circulation in the Indian Ocean, as marked as "approximate cut-off" in Fig. 2, and as described above. This type of disconnection would allow the Indo-Atlantic and Pacific Oceans to evolve differently. We offer, nevertheless, two important qualifications with respect to this interpretation of the PETM oceans. First, we are fully cognizant that there exist sites to the east of our proposed Indian Ocean cut-off line (notably DSDP Site 213), that show evidence of extensive $CaCO_3$ dissolution during the PETM (Slotnick et al., 2015). As remarked above, the position of the cut-off should be considered approximate, but the existence of a barrier (somewhere) is supported by the neodymium isotopic data. In addition, the (Indo-)Pacific was subject to its own, if less intense, acidification i.e., at least 1000 GtC were input to that ocean. What we are then advocating, at a minimum, is a singular lack of Pacific water flow into the Indo-Atlantic, as any appreciable water input from that larger ocean creates a buffering that stops the development of the degree of under-saturation needed to explain the Walvis Ridge data.

All the results given above contain one other commonality. Fig. 8A shows the $CaCO_3$ time series and our model prediction, i.e., blue line, at 1500 m paleo-depth at Walvis Ridge obtained with constant net $CaCO_3$ production from the surface waters, i.e., B_A in Fig. 3; that prediction never falls below 65% $CaCO_3$. Fig. 8B illustrates the corresponding hindcast at 3600 m, and the mismatch of the blue line with the data is extreme with respect to timing and over-shooting. To obtain acceptable concordance at 1500 m, i.e., the red line, the calcite rain to the deep sea at Walvis Ridge must have been ∼50% lower during the first 70 ka PO, only to recover gradually to the initial value at about 100 ka PO. This reduced net productivity has already been included in all our earlier reported results in Figs. 4–7; in fact, we tested a wide range of combinations of CO_2 release, inter-ocean exchange and export changes to arrive at our optimum results in Figs. 7 and 8 as the red lines.

To re-emphasize, once a simulation of the $CaCO_3$ time series for 1500 m has been created, the generated model outputs for 2600 and 3600 m paleo-depths are retrodictions, i.e., no adjustable parameters are left in the model to force a fit. Without a reduction in $CaCO_3$ export, our model (blue line in Fig. 8B) predicts that $CaCO_3$-free sediment would continue to accumulate at 3600 m for another ∼20 ka after CO_2 input ceased, followed then by a monotonic increase of $CaCO_3$ towards the pre-PETM values, all of which disagrees with the data. The same is true at 2600 m (results not shown). With a temporary 50% reduction in $CaCO_3$ export, our

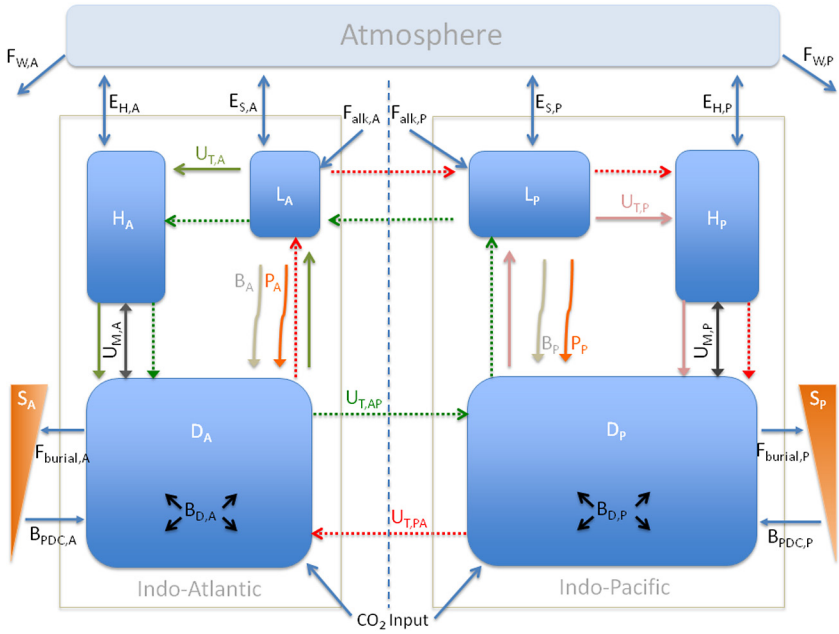

Fig. 3. Our box model for the carbonate system of the PETM oceans, and the fluxes that operate between the reservoirs. The model divides the oceans into a collection of 6 boxes, i.e., High Latitude Indo-Atlantic (H_A), Low Latitude Surface Indo-Atlantic (L_A), Deep Indo-Atlantic (D_A), High Latitude Pacific (H_P), Low Latitude Surface Pacific (L_P), and Deep Pacific (D_P), as well as an atmospheric box and 2 sediment reservoirs connected to the deep water boxes. Possible water flows between boxes are designated by capital U's, the capital E's indicate gas exchanges, the B's stand for internal fluxes of $CaCO_3$, and the F's are the external fluxes of carbonate alkalinity to the surface boxes or of $CaCO_3$ to the sediments. Subscripts refer to the particular ocean (A and P) and the nature of the flux, e.g., T for thermohaline, M for mixing, D for dissolution, burial for sedimentation of $CaCO_3$, alk for the alkalinity input from rivers, W for CO_2 return to the erosion cycle, etc. Solid lines with arrows indicate fluxes that are always active; dashed lines are fluxes that are shut off during our simulations, e.g., exchange between the Indo-Atlantic and the Pacific deep waters. Rather than placing labels on every single flow, we use colors and line type (solid versus dashed) to identify flows that are the same, but attached to different boxes, e.g., thermohaline flow solely within the Indo-Atlantic is given by solid olive green arrows (3 of them between the Indo-Atlantic boxes), while a thermohaline flow that originates in the Indo-Atlantic and goes to the Pacific is indicated by dashed green arrows (5 of them), etc. The CO_2 input into the deep oceans is indicated by the "CO_2 input" labeled arrows at the base of the diagram. Note previously deposited $CaCO_3$ can dissolve if the bottom waters become more acidic. The equations for this model are described in Appendix A, as well as initial values for these flows, except if they are model outputs, i.e., F_{burial}, B_{PDC}, F_W and all the E values.

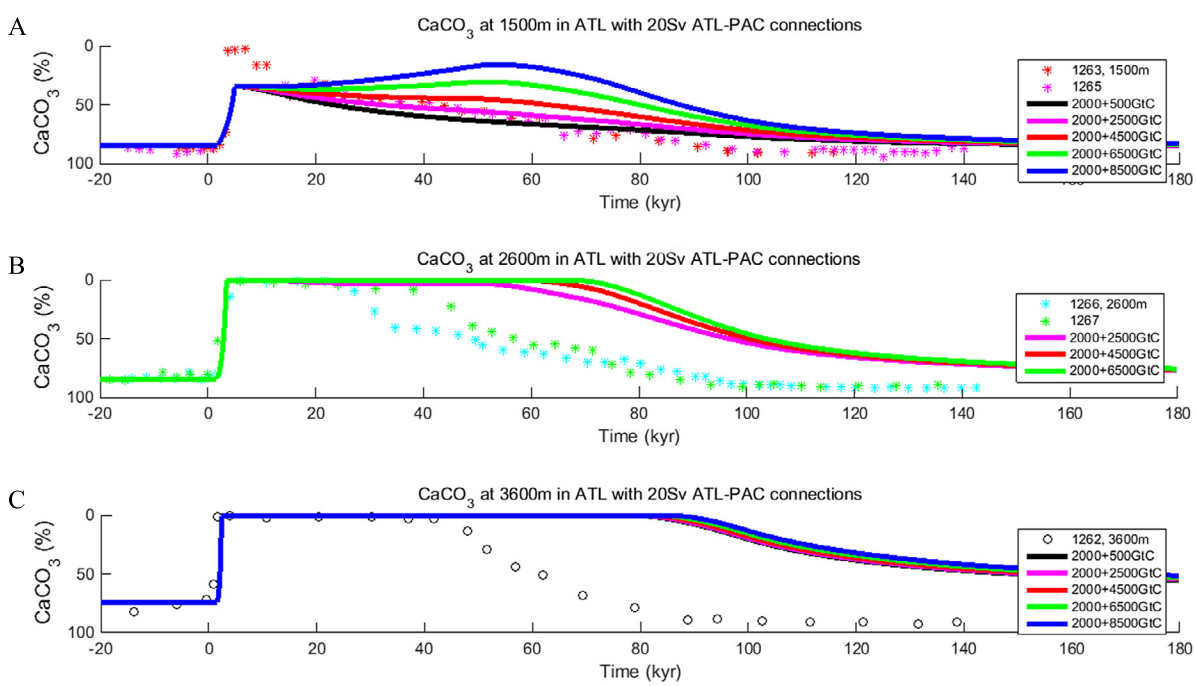

Fig. 4. A comparison of $CaCO_3$ records (time series) on the Walvis Ridge and our model predictions for 20 Sv of deep-water exchange between the Indo-Atlantic and Pacific Oceans. The data are given as colored symbols and the predictions are the solid lines. The color of the lines indicate different amounts of CO_2 released into the oceans during the PETM, which occurred in two phases (Zeebe et al., 2009), one of 5 kyr duration, followed by one of 50 kyr duration. For example the red line in all panels is generated with an initial 2000 GtC release, than a 4500 GtC release. **A.** Data and model results for at 1500 m paleo-depth. **B.** Data and model results for at 2600 m paleo-depth. **C.** Data and model results for at 2600 m paleo-depth. This is repeated in the next 3 figures.

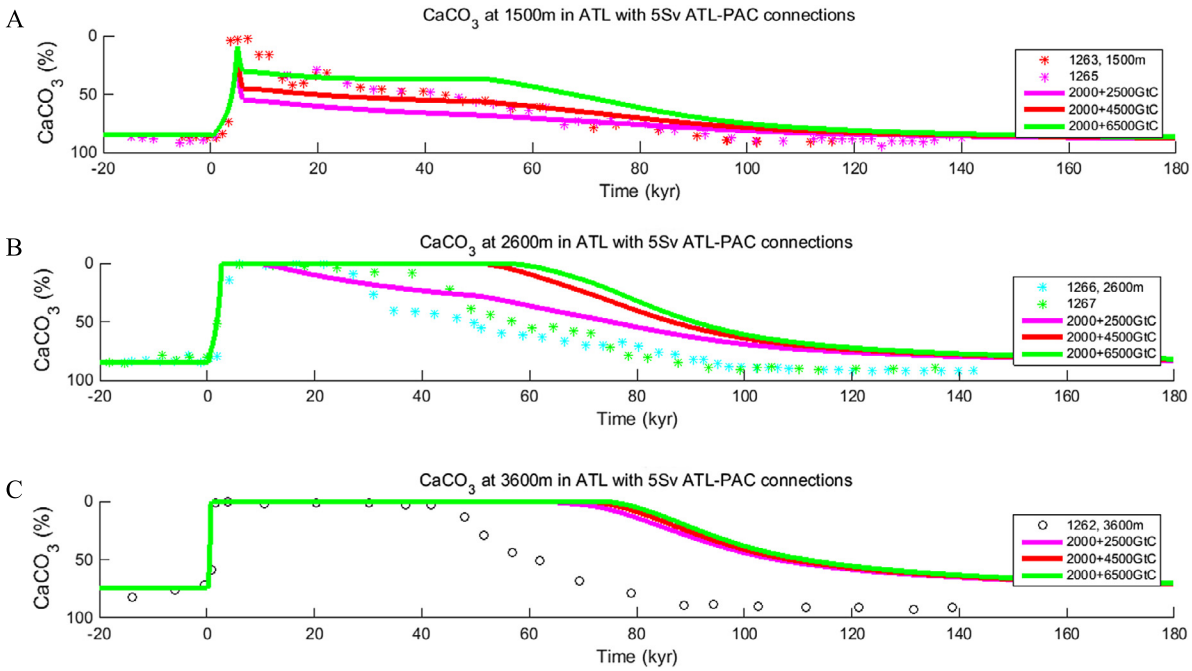

Fig. 5. A comparison of $CaCO_3$ records (time series) on the Walvis Ridge and our model predictions for 5 Sv of deep-water exchange between the Indo-Atlantic and Pacific Oceans. **A**. Data and model results for at 1500 m paleo-depth. **B**. Data and model results for at 2600 m paleo-depth. **C**. Data and model results for at 2600 m paleo-depth.

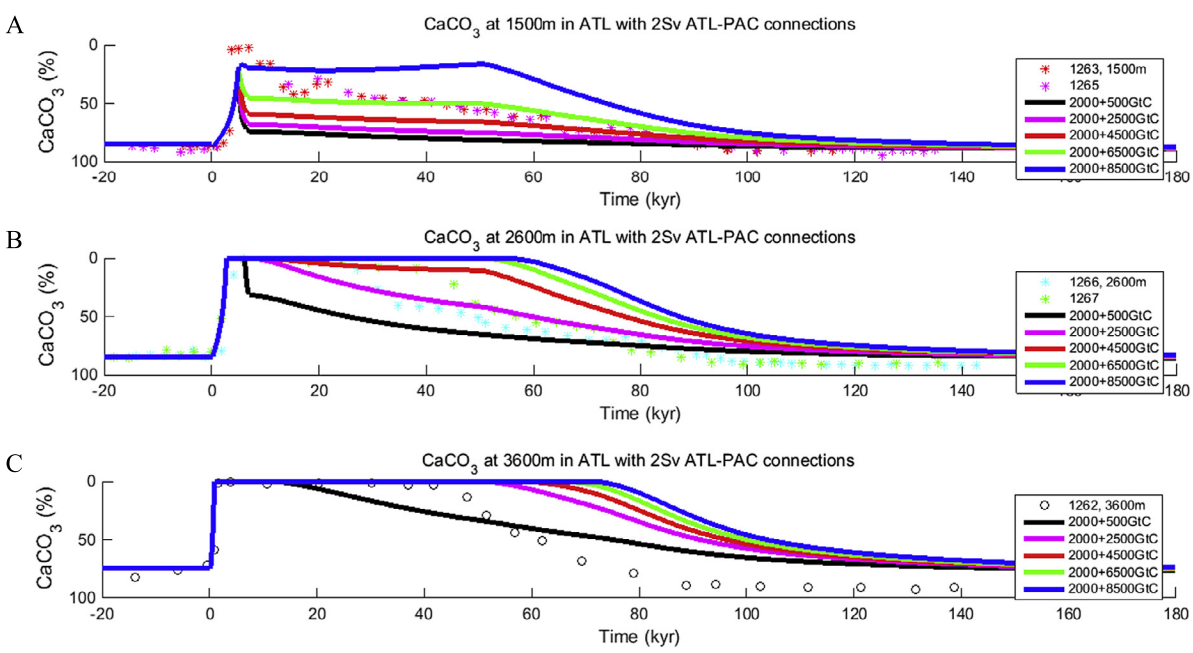

Fig. 6. A comparison of $CaCO_3$ records (time series) on the Walvis Ridge and our model predictions for 2 Sv of deep-water exchange between the Indo-Atlantic and Pacific Oceans. **A**. Data and model results for at 1500 m paleo-depth. **B**. Data and model results for at 2600 m paleo-depth. **C**. Data and model results for at 2600 m paleo-depth.

model predicts a trend close to the data at all paleo-depths, i.e. red lines in Figs. 7 and 8.

A ∼50% drop in net $CaCO_3$ production could indicate either a fall in $CaCO_3$ production itself or a temporary increase in near-surface dissolution (i.e., in surface and in pycnocline waters). Dissolution in supersaturated surface and pycnocline waters is still not well understood from a mechanistic point of view and it is not known how it responds to changes in ocean acidity; consequently, we chose to ignore this possibility and focus on changing $CaCO_3$ productivity. Even restricting ourselves to changing productivity, such alterations could occur at constant or variable B to P (PIC/POC) ratio. While we did examine independent B and P changes, all results reported here are for constant P.

With respect to changing net productivity, there are no independent estimates of B for the Walvis Ridge sites to check our result, but Gibbs et al. (2010) – see their Fig. 3A, panel 4 – estimate a 20–25% drop in $CaCO_3$ productivity at ODP Site 690 in the Southern Ocean during most of the early PETM. ODP Site 690 was likely not as oligotrophic as Walvis Ridge (Nicolo et al., 2010), where we might expect an even greater drop.

Surprisingly, our optimum model result with reduced net $CaCO_3$ productivity displays over-deepening without any intervention on

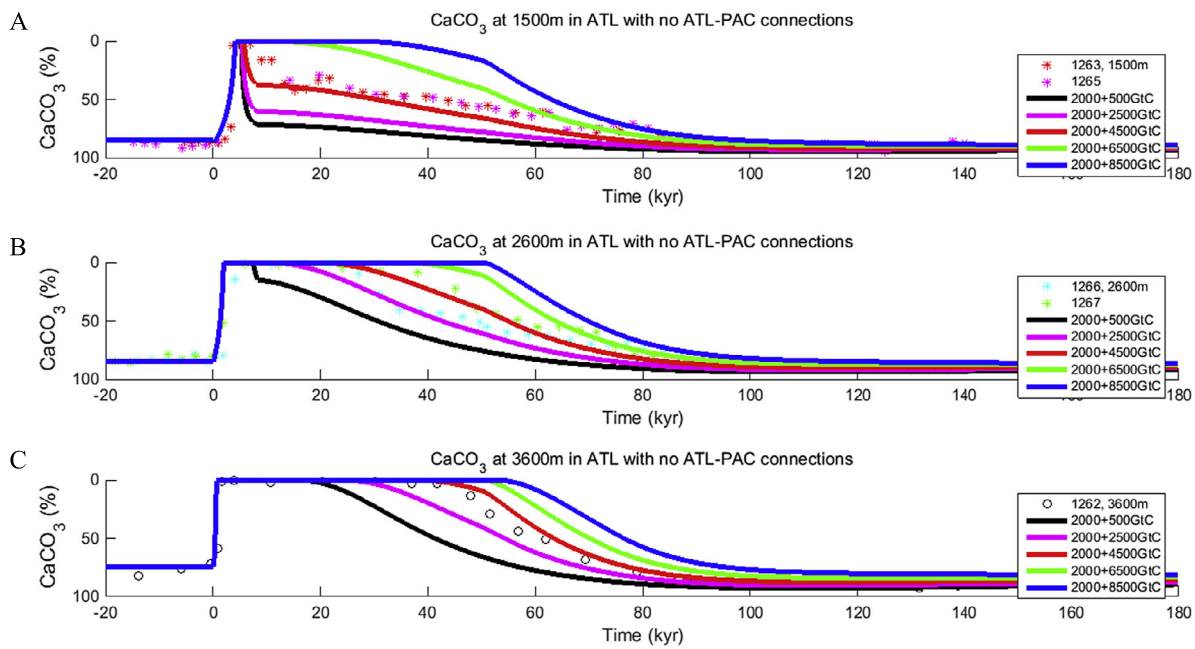

Fig. 7. A comparison of $CaCO_3$ records (time series) on the Walvis Ridge and our model predictions for 0 Sv of deep-water exchange between the Indo-Atlantic and Pacific Oceans (complete isolation). **A**. Data and model results for at 1500 m paleo-depth. **B**. Data and model results for at 2600 m paleo-depth. **C**. Data and model results for at 2600 m paleo-depth.

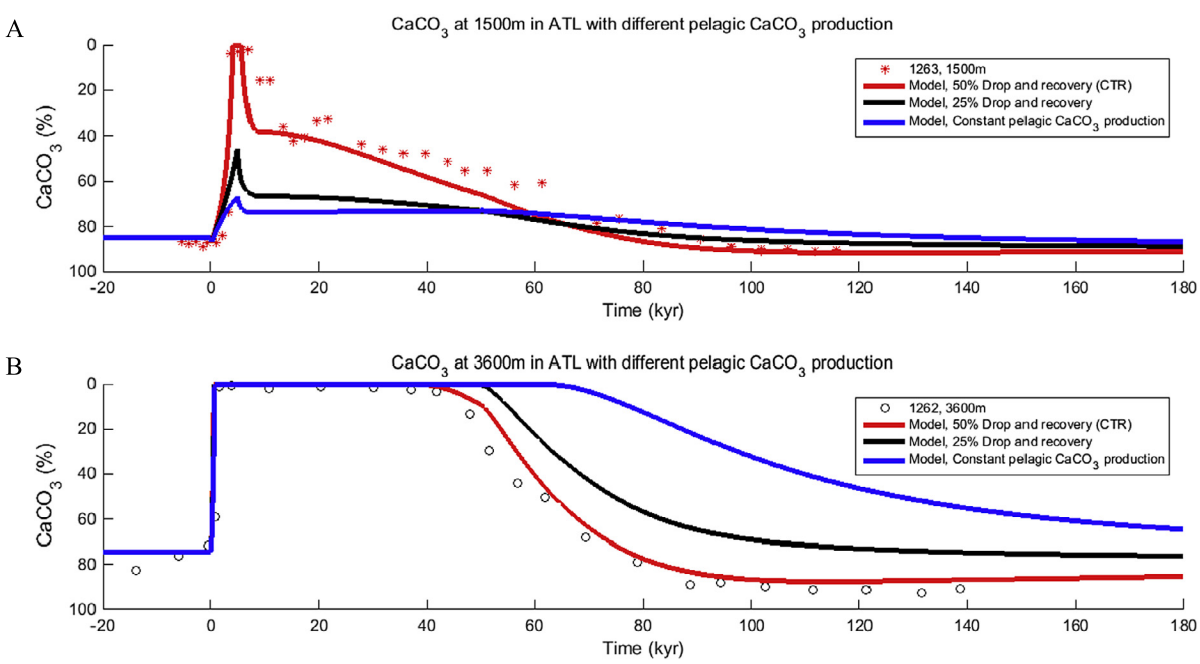

Fig. 8. A comparison of $CaCO_3$ records on the Walvis Ridge and model predictions as functions of the rate of net $CaCO_3$ production from the surface waters to the deep oceans. **A** shows the data and prediction at 1500 m, while **B** illustrates the same at 3600 m. The best correspondence with the data is obtained with ∼50% reduction in net production and is given by the red curve, which is also the red curve in Fig. 7.

our part (Fig. 8) and including a constant riverine alkalinity input. For over-deepening to occur in the deep Indo-Atlantic Ocean, that water must eventually become more saturated than it was before the PETM. Even though the PETM is correctly considered an acidification event, there must have been later alkalinization of the deep Indo-Atlantic Ocean and, possibly to a lesser extent, in the Pacific.

This alkalinization has previously been attributed to increased riverine input of bi-carbonate (e.g., Zachos et al., 2005; Kump et al., 2009; Zeebe and Zachos, 2013; Penman et al., 2016). In a steady state, alkalinity input from rivers (F_{alk} in Fig. 3) is removed by production and burial of $CaCO_3$. Thus, an increase in the riverine alkalinity input, at constant productivity, leads to an increase in dissolved CO_3^{2-} and deep-water saturation, which in turn increases the burial (survival) of $CaCO_3$ to counteract that added alkalinity input (Zachos et al., 2005). The net result is deeper preservation of $CaCO_3$. Nonetheless, our results (Figs. 7 & 8) suggest an alternative mechanism, which can operate with or without increased weathering; this alternative is offered without prejudice to any actual increased weathering that there might have been during the PETM. Specifically, we advance that the traditional (canonical) view of carbonate compensation is too restrictive and needs

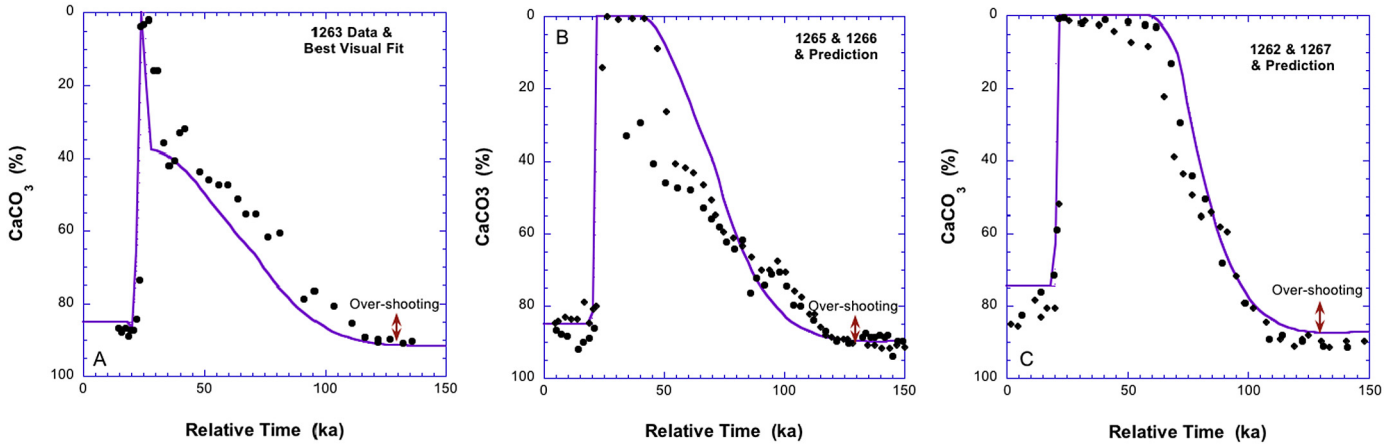

Fig. 9. A summary of the best correspondence between the results of our model and the $CaCO_3$ data from the Walvis Ridge sites. Note the improvements in magnitude and timing at all depths with respect to the acidification phase, as compared to the predictions by others in Fig. 1, and the presence of over-shooting, again at all paleo-depths, caused by biological carbonate compensation.

to be extended to account for the possibility of biologically driven net $CaCO_3$ production feedbacks, as advocated earlier by Zeebe and Westbroek (2003).

To illuminate the importance of this additional feedback mechanism to acidification, consider the steady-state alkalinity balance for an ocean, i.e.,

$$F_{alk}/2 = B - B_D \quad (2)$$

where B is the rate of net $CaCO_3$ production, B_D is the total rate of dissolution in the deep ocean (see Boudreau et al., 2010b; Appendix A), and F_{alk} is the input of carbonate alkalinity to the ocean. Note that the difference $B - B_D$ is also the burial rate of $CaCO_3$, regardless of the presence or absence of a steady state. If extra CO_2 is now injected into this ocean, while F_{alk} and B remain constant, e.g., as in Zachos et al. (2005), Zeebe and Zachos (2007), Panchuk et al. (2008), and Zeebe et al. (2009), then CO_3^{2-} will first fall, dissolution B_D will increase because it is a function of the CO_3^{2-}, and burial $(B - B_D)$ will decrease. The added $CaCO_3$ dissolution releases carbonate ion into the ocean, which thereafter neutralizes the added CO_2, as summarized by reaction (1), above. This sequence constitutes canonical carbonate compensation, as exemplified by the blue lines in Fig. 8, which do not explain the data (without increased weathering).

Alternatively, if net productivity B falls as a result of CO_2 input, and B_D remains initially the same, there will be less burial and less alkalinity removal. If B_D increases too, then there will be even less burial and alkalinity removal. Thus, with constant F_{alk}, the reduced (net) burial $(B - B_D)$ would produce a build-up of alkalinity. For example, with B at ∼50% of the pre-PETM condition in the Indo-Atlantic (Appendix A, Fig. A3), the burial rate in the first 70 kyr is no greater than half of that with constant B – see Appendix A, Fig. A4. The unbalanced input of alkalinity causes CO_3^{2-} to accumulate to values greater than pre-PETM conditions, carbonate saturation becomes even greater, and more $CaCO_3$ can accumulate at every depth. Canonical carbonate compensation continues to occur at the same time as this additional effect. Thus, using this mechanism, from about ∼90 ka PO onward, the sediments at all three paleo-depths start to accumulate more $CaCO_3$ than before the PETM, producing over-deepening, as shown in Fig. 8. Even with full recovery of B from 100 ka PO onward, the excess alkalinity is not eliminated as late as 150 ka PO and the over-deepened state persists.

The added role of net $CaCO_3$ productivity in the above scenario constitutes an important modification that we term *biological* carbonate compensation. The final optimum results of our modeling are displayed in Fig. 9, and these are visually superior in all respects, i.e., magnitude, timing and over-shooting, than those provided by either Ridgwell (2007) or Zeebe et al. (2009), as displayed in Fig. 2. (Statistics on these fits are in Appendix A for those who are interested.)

Canonical carbonate compensation figures prominently in buffering the carbonate chemistry of the oceans, in part, because of its symmetric operation. With acidification, the dissolution of a greater proportion of the $CaCO_3$ productivity and of previously deposited $CaCO_3$ returns the ocean towards its original state. We can see from the above discussion that reduced production with biological compensation during acidification will cause a parallel return towards the pre-perturbation state. Conversely, with alkalinization, canonical compensation causes added preservation (B_D is smaller), which reduces the alkalinity, again to move the ocean towards a previous state. If higher carbonate saturation levels promote planktonic calcification (e.g., Lea et al., 1995; Comeau et al., 2010; Bach et al., 2015; Meyer and Riebesell, 2015), then this would have the same effect as canonical compensation by supplying more $CaCO_3$ for burial, thus reducing the alkalinity of ocean waters. The end-result symmetry between the two forms of compensation would then be complete. This suggests that research into *in situ* calcification at increased saturation (pH) would be valuable in establishing biological carbonate compensation as a process that could rival canonical compensation.

Before ending this section, we note that an attenuated feedback between $CaCO_3$ export and acidification has been included in two other previous models, but without discovering its importance. Ridgwell and Hargreaves (2007) did not run their model far enough into the Eocene after acidification to observe over-shooting (Fig. 1). Lord et al. (2015) also had such a mechanism in their model, but ran their results with a weathering feedback that camouflaged the effects of biological carbonate compensation.

5. Conclusions and future research

Our simulations of the PETM $CaCO_3$ records at Walvis Ridge ODP sites (Fig. 9) were obtained, in part, by limiting deep-water two-way exchange between the Indo-Atlantic and Pacific Oceans (Figs. 4–7) and reducing by ∼50% the net production of $CaCO_3$ during acidification (Fig. 8), two conditions not considered (fully) in previous models. In addition, these $CaCO_3$ records are best reproduced with the introduction of a *maximum* of ∼6500 GtC of CO_2 directly into deep-ocean waters or ∼8000 GtC into the atmosphere (Appendix A).

The proposed loss of net $CaCO_3$ production caused a build-up of alkalinity in the deep-waters of the Indo-Atlantic Ocean, and

restoration of net $CaCO_3$ production later in the PETM led to overshooting, as the $CaCO_3$ tests then fell into waters more saturated than before the start of the PETM.

These findings prompt us to propose an extension of the concept of carbonate compensation to include biological carbonate compensation. It should include not only the canonical idea of increased dissolution of $CaCO_3$ reaching the seafloor and of previously deposited $CaCO_3$ in response to acidification, but also the concept that a reduction in biological calcification will decrease the removal of alkalinity, allowing it to build-up, thus re-adjusting the benthic saturation state, so as to compensate for the addition of CO_2.

There is evidence for enhanced physical weathering during the PETM. Given the nominally 5 °C warming across this event, one might expect that the PETM may also have been a period of enhanced chemical weathering with a consequently greater riverine alkalinity flux. The latter could also lead to over-shooting. Whether increased weathering or biological carbonate compensation dominates should be a question for future research. Detailed records of deep-sea carbonate accumulation across the PETM at multiple, contiguous locations, especially in the Pacific, would aid greatly and constrain future modeling.

Acknowledgements

YL and BPB gratefully acknowledge funding from NSERC. JJM and AS were supported by the Netherlands Earth System Science Center (NESSC). This research used samples and/or data provided by the International Ocean Discovery Program (IODP). AS thanks the European Research Council (ERC) for Starting Grant 259627. GRD acknowledges funding from a US NSF Frontiers grant (NSF-FESD-OCE-1338842). We enjoyed fruitful discussions with Markus Kienast and Paul Hill (both at Dalhousie University) on various aspects of this paper. We thank Karen Bice for access to her bathymetric data. We thank, our editor, Heather Stoll, as well as Andy Ridgwell and two anonymous reviewers for particularly useful reviews. All (real) data in this paper are taken from the cited papers, and the code that generated our hindcasts is available from BPB.

Appendix. Supplementary material

Supplementary material related to this article can be found online at http://dx.doi.org/10.1016/j.epsl.2016.08.012.

References

Abbott, A.N., Haley, B.A., Tripati, A.K., Frank, M., 2016. Constraints on ocean circulation at the Paleocene–Eocene Thermal Maximum from neodymium isotopes. Clim. Past 12, 837–847. http://dx.doi.org/10.5194/cp-12-837-2016; www.clim-past.net/12/837/2016.

Alexander, K., Meissner, K.J., Bralower, T.J., 2015. Sudden spreading of corrosive bottom water during the Palaeocene–Eocene Thermal Maximum. Nat. Geosci. 8, 458–461. http://dx.doi.org/10.1038/NGEO2430.

Archer, D., Eby, M., Brovkin, V., Ridgwell, A., Cao, L., Mikolajewicz, U., Caldeira, K., Matsumoto, K., Munhoven, G., Montenegro, A., Tokos, K., 2009. Atmospheric lifetime of fossil fuel carbon dioxide. Annu. Rev. Earth Planet. Sci. 37, 117–134. http://dx.doi.org/10.1146/annurev.earth.031208.100206.

Baatsen, M., van Hinsbergen, D.J.J., von der Heydt, A.S., Dijkstra, H.A., Sluijs, A., Abels, H.A., Bijl, P.K., 2016. A generalised approach to reconstructing geographical boundary conditions for palaeoclimate modelling. Clim. Past 12, 1635–1644. http://dx.doi.org/10.5194/cp-12-1635-2016.

Bach, L.T., Riebesell, U., Gutowska, M.A., Federwisch, L., Schulz, K.G., 2015. A unifying concept of coccolithophore sensitivity to changing carbonate chemistry embedded in an ecological framework. Prog. Oceanogr. 135, 125–138. http://dx.doi.org/10.1016/j.pocean.2015.04.012.

Bice, K.L., Marotzke, J., 2001. Numerical evidence against reversed thermohaline circulation in the warm Paleocene/Eocene ocean. J. Geophys. Res. 106, 11529–11542.

Boudreau, B.P., Middelburg, J.J., Meysman, F.J.R., 2010a. Carbonate compensation dynamics. Geophys. Res. Lett. 37, L03603. http://dx.doi.org/10.1029/2009GL041847.

Boudreau, B.P., Middelburg, J.J., Hoffmann, A.F., Meysman, F.J.R., 2010b. Ongoing transients in carbonate compensation. Glob. Biogeochem. Cycles 24, GB4010. http://dx.doi.org/10.1029/2009GB003654.

Bralower, T.J., Kelly, D.C., Gibbs, S., Farley, K., Eccles, L., Lindemann, T.L., Smith, G.J., 2014. Impact of dissolution on the sedimentary record of the Paleocene–Eocene thermal maximum. Earth Planet. Sci. Lett. 401, 70–82.

Carozza, D.A., Mysak, L.A., Schmidt, G.A., 2011. Methane and environmental change during the Paleocene–Eocene thermal maximum (PETM): modeling the PETM onset as a two-stage event. Geophys. Res. Lett. 38, L05702. http://dx.doi.org/10.1029/2010GL046038.

Comeau, S., Jeffree, R., Teyssié, J.-L., Gattuso, J.-P., 2010. Response of the arctic pteropod limacina helicina to projected future environmental conditions. PLoS ONE 5, e11362. http://dx.doi.org/10.1371/journal.pone.0011362.

Cui, Y., Kump, L.R., Ridgwell, A.J., Charles, A.J., Junium, C.K., Diefendorf, A.F., Freeman, K.H., Urban, N.M., Harding, I.C., 2011. Slow release of fossil carbon during the Palaeocene–Eocene Thermal Maximum. Nat. Geosci. 4, 481–485.

DeConto, R.M., Galeotti, S., Pagani, M., Tracy, D., Schaefer, K., Zhang, T., Pollard, D., Beerling, D.J., 2012. Past extreme warming events linked to massive carbon release from thawing permafrost. Nature 484, 87–92.

Dickens, G.R., 2001. Carbon addition and removal during the Late Palaeocene Thermal Maximum: basic theory with a preliminary treatment of the isotope record at ODP Site 1051, Blake Nose. Geol. Soc. (Lond.) Spec. Publ. 183, 293–305.

Dickens, G.R., Castillo, M.M., Walker, J.C.G., 1997. A blast of gas in the latest Paleocene: simulating first-order effects of massive dissociation of oceanic methane hydrate. Geology 25, 259–262.

Dickens, G.R., O'Neil, J.R., Rea, D.K., Owen, R.M., 1995. Dissociation of oceanic methane hydrate as a cause of the carbon isotope excursion at the end of the Paleocene. Paleoceanography 10, 965–971.

Gibbs, S.J., Stoll, H.M., Bown, P.R., Bralower, T.J., 2010. Ocean acidification and surface water carbonate production across the Paleocene–Eocene thermal maximum. Earth Planet. Sci. Lett. 295, 583–592.

Heinze, M., Ilyana, T., 2015. Ocean biogeochemistry in the warm climate of the late Paleocene. Clim. Past 11, 63–79. http://dx.doi.org/10.5194/cp-11-63-2015.

Herold, N., Buzan, J., Seton, M., Goldner, A., Green, J.A.M., Müller, R.D., Markwick, P., Huber, M., 2014. A suite of early Eocene (∼55 Ma) climate model boundary conditions. Geosci. Model Dev. 7, 2077–2090.

Kelly, D.C., Neilsen, T.M.J., McCarren, H.K., Zachos, J.C., Röhl, U., 2010. Spatiotemporal patterns of carbonate sedimentation in the South Atlantic: implications for carbon cycling during the Paleocene–Eocene Thermal Maximum. Palaeogeogr. Palaeoclimatol. Palaeoecol. 293, 30–40.

Kump, L.R., Bralower, T.J., Ridgwell, A., 2009. Ocean acidification in deep time. Oceanography 22, 94–107.

Lea, D.W., Martin, P.A., Chan, D.A., Spero, H.J., 1995. Calcium uptake and calcification rate in the planktonic foraminifer *Orbulina universa*. J. Foraminiferal Res. 25, 14–23.

Leon-Rodriguez, L., Dickens, G.R., 2010. Constraints on ocean acidification associated with rapid and massive carbon injections: the early Paleogene record at ocean drilling program site 1215, equatorial Pacific Ocean. Palaeogeogr. Palaeoclimatol. Palaeoecol. 298, 409–420.

Lord, N.S., Ridgwell, A., Thorne, M.C., Lunt, D.J., 2015. An impulse response function for the "long tail" of excess atmospheric CO_2 in an Earth system model. Glob. Biogeochem. Cycles 29. http://dx.doi.org/10.1002/2014GB005074.

McInerney, F.A., Wing, S.L., 2011. The Palaeocene–Eocene Thermal Maximum: a perturbation of carbon cycle, climate, and biosphere with implications for the future. Annu. Rev. Earth Planet. Sci. 39, 489–516.

Meyer, J., Riebesell, U., 2015. Reviews and syntheses: responses of coccolithophores to ocean acidification: a meta-analysis. Biogeosciences 12, 1671–1682. http://dx.doi.org/10.5194/bg-12-1671-2015.

Montes, C., Cardona, A., McFadden, R., Morón, S.E., Silva, C.A., Restrepo-Moreno, S., Ramírez, D.A., Hoyos, N., Wilson, J., Farris, D., Bayona, G.A., Jaramillo, C.A., Valencia, V., Bryan, J., Flores, J.A., 2012. Evidence for middle Eocene and younger land emergence in central Panama: implications for Isthmus closure. Geol. Soc. Am. Bull. 124, 780–799. http://dx.doi.org/10.1130/B30528.1.

Nicolo, M.J., Dickens, G.R., Hollis, C.J., 2010. South Pacific intermediate water oxygen depletion at the onset of the Paleocene–Eocene thermal maximum as depicted in New Zealand margin sections. Paleoceanography 25, PA4210. http://dx.doi.org/10.1029/2009PA001904.

Nobre Silva, I.G., Weis, D., Scoates, J.S., Barling, J., 2013. The Ninetyeast Ridge and its relation to the Kerguelen, Amsterdam and St. Paul Hotspots in the Indian Ocean. J. Petrol. 54, 1177–1220.

Orr, J.C., Fabry, V.J., Aumont, O., Bopp, L., Doney, S.C., Feely, R.A., Gnanadesikan, A., Gruber, N., Ishida, A., Joos, F., Key, R.M., Lindsay, K., Maier-Reimer, E., Matear, R., Monfray, P., Mouchet, A., Najjar, R.G., Plattner, G.-K., Rodgers, K.B., Sabine, C.L., Sarmiento, J.L., Schlitzer, R., Slater, R.D., Totterdell, I.J., Weirig, M.-F., Yamanaka, Y., Yool, A., 2005. Anthropogenic ocean acidification over the twenty-first century and its impact on calcifying organisms. Nature 437, 681–686.

Panchuk, K., Ridgwell, A., Kump, L.R., 2008. Sedimentary response to Paleocene–Eocene Thermal Maximum carbon release: a model-data comparison. Geology 36, 315–318.

Penman, D.E., Turner, S.K., Sexton, P.F., Norris, R.D., Dickson, A.J., Boulila, S., Ridgwell, A., Zeebe, R.E., Zachos, J.C., Cameron, A., Westerhold, T., Röhl,

U., 2016. An abyssal carbonate compensation depth overshoot in the aftermath of the Palaeocene–Eocene Thermal Maximum. Nat. Geosci. 9, 575–580. http://dx.doi.org/10.1038/ngeo2757.

Ravizza, G., Norris, R.N., Blusztajn, J., Aubry, M.P., 2001. An osmium isotope excursion associated with the Late Paleocene thermal maximum: evidence of intensified chemical weathering. Paleoceanography 16, 155–163.

Ridgwell, A., 2007. Interpreting transient carbonate compensation depth changes by marine sediment core modeling. Paleoceanography 22, PA4102. http://dx.doi.org/10.1029/2006PA001372.

Ridgwell, A., Hargreaves, J.C., 2007. Regulation of atmospheric CO_2 by deep-sea sediments in an Earth system model. Glob. Biogeochem. Cycles 21, GB2008. http://dx.doi.org/10.1029/2006GB002764.

Riebesell, U., 2008. Acid test for marine biodiversity. Nature 454, 46–47.

Riebesell, U., Zondervan, I., Rost, B., Tortell, P.D., Zeebe, R.E., Morel, F.M.M., 2000. Reduced calcification of marine plankton in response to increased atmospheric CO_2. Nature 407, 364–367.

Scher, H.D., Martin, E.E., 2006. Timing and climatic consequences of the opening of Drake passage. Science 312, 628–630.

Slotnick, B.S., Lauretano, V., Backman, J., Dickens, G.R., Sluijs, A., Loutens, L., 2015. Early Paleogene variations in the calcite compensation depth: new constraints using old borehole sediments from across Ninetyeast Ridge, central Indian Ocean. Clim. Past 11, 473–493.

Thomas, D.J., Bralower, T.J., Jones, C.E., 2003. Neodymium isotopic reconstruction of the Paleocene–early Eocene thermohaline circulation. Earth Planet. Sci. Lett. 209, 309–322.

Waldbusser, G.G., Hales, B., Langdon, C.J., Haley, B.A., Schrader, P., Brunner, E.L., Gray, M.W., Miller, C.A., Gimenez, I., 2014. Saturation-state sensitivity of marine bivalve larvae to ocean acidification. Nat. Clim. Change. http://dx.doi.org/10.1038/nclimate2479.

Wallace, P.J., Frey, F.A., Weis, D., Coffin, M.F., 2002. Origin and evolution of the Kerguelen Plateau, Broken Ridge and Kerguelen Archipelago: editorial. J. Petrol. 43, 1105–1108.

Wegner, W., Wörner, G., Harmon, M.E., Jicha, B.R., 2011. Magmatic history and evolution of the Central American land bridge in Panama since the Cretaceous times. Geol. Soc. Am. Bull. 123, 703–724.

Weis, D., Frey, F.A., Saunders, S.A., Gibson, I., 1991. Leg 121 Shipboard Scientific Party, 1991. The Ninetyeast Ridge (Indian Ocean): a 5000 km record of a DUPAL mantle plume. Geology 19, 99–102.

Weissel, J., Peirce, J., Taylor, E., Alt, J., et al. (Eds.), 1991. Proceedings of the Ocean Drilling Program: Scientific Results, vol. 121. College Station, TX (Ocean Drilling Program).

Zachos, J.C., Rohl, U., Schellenberg, S.A., Sluijs, A., Hodell, D.A., Kelly, D.C., Thomas, E., Nicolo, M., Raffi, I., Lourens, L.J., McCarren, H., Kroon, D., 2005. Rapid acidification of the ocean during the Palaeocene–Eocene Thermal Maximum. Science 308, 1611–1615.

Zeebe, R.E., Ridgwell, A., 2011. Past changes in ocean carbonate chemistry. In: Gattuso, J.P., Hansson, L. (Eds.), Ocean Acidification. Oxford University Press, Oxford, pp. 21–40.

Zeebe, R.E., Westbroek, P.A., 2003. A simple model for the $CaCO_3$ saturation state of the ocean: the "strangelove", the "Neritan", and the "Cretan" ocean. Geochem. Geophys. Geosyst. 4, 1104. http://dx.doi.org/10.1029/2003GC000538.

Zeebe, R.E., Zachos, J.C., 2007. Reversed deep-sea carbonate ion basin gradient during the Paleocene–Eocene thermal maximum. Paleoceanography 22, PA3201. http://dx.doi.org/10.1029/2006PA001395.

Zeebe, R.E., Zachos, J.C., 2013. Long-term legacy of massive carbon input to the Earth system: Anthropocene versus Eocene. Philos. Trans. R. Soc. A 371, 20120006. http://dx.doi.org/10.1098/rsta.2012.0006.

Zeebe, R.E., Zachos, J.C., Dickens, G.R., 2009. Carbon dioxide forcing alone insufficient to explain Palaeocene–Eocene Thermal Maximum warming. Nat. Geosci. 2, 576–580.